WDM multi-channel silicon photonic receiver with 320 Gbps data transmission capability

Qing Fang,[1,*] Tsung-Yang Liow,[1] Jun Feng Song,[1,2] Kah Wee Ang,[1] Ming Bin Yu,[1] Guo Qiang Lo,[1] and Dim-Lee Kwong[1]

[1]*Institute of Microelectronics, A*STAR (Agency for Science, Technology and Research), 11 Science Park Road, Singapore Science Park II, 117685, Singapore.*

[2]*State Key Laboratory on Integrated Opto-electronics, College of Electronic Science and Engineering, Jilin University, Changchun, 130023, China.*

**Fangq@ime.a-star.edu.sg*

Abstract: A high performance monolithically integrated WDM receiver is fabricated on the SOI platform, with key components comprising a 1 x 32 Si-based AWG and an array of high speed waveguided Ge-on-Si photodetectors. The optical channel spacing is 200 GHz. This configuration was used to demonstrate 32-channel operation in the L-band, where it is particularly challenging for silicon photonics due to the low absorption coefficient of Ge at L-band wavelengths. Each channel is capable of operating at a data rate of at least 10 Gbps, resulting in an aggregate data rate of 320 Gbps. At a BER of 1×10^{-11}, the WDM receiver showed an optical input sensitivity between −16 dBm and −19 dBm.

OCIS Codes: (130.3120) Integrated optics devices; (130.0250) Optoelectronics; (130.2990) Semiconductors; (130.2790) Guided waves; (220.0220) Optical design and fabrication

References and links:

1. Q. Xu, B. Schmidt, J. Shakya, and M. Lipson, "Cascaded silicon micro-ring modulators for WDM optical interconnection," Opt. Express **14**(20), 9431–9435 (2006).
2. G. Jacobsen, and P. Wildhagen, "A general and rigorous WDM receiver model targeting 10-40-Gb/s channel bit rates," J. Lightwave Technol. **19**(7), 966–976 (2001).
3. B. G. Lee, B. A. Small, Q. Xu, M. Lipson, and K. Bergman, "Characterization of a 4 × 4 Gb/s parallel electronic bus to WDM optical link silicon photonic translator," IEEE Photon. Technol. Lett. **19**(7), 456–458 (2007).
4. T. Ohyama, Y. Akahori, T. Yamada, R. Kasahara, S. Kamei, M. Ishii, M. Nakamura, H. Oohashi, N. Matsuura, and K. Yamakoshi, "Compact 8-wavelength × 2.5 Gbit/s transmitter/receiver module using PLC hybrid integration technology for WDM interconnections," Electron. Lett. **38**(24), 1576–1578 (2002).
5. Y.-T. Han, Y.-J. Park, S.-H. Park, J.-U. Shin, D.-J. Kim, S.-W. Park, S.-H. Song, K.-Y. Jung, D.-J. Lee, W.-Y. Hwang, and H.-K. Sung, "1.25-Gb/s bidirectional transceiver module using 1.5%-Δ silica directional coupler-type WDM," IEEE Photon. Technol. Lett. **17**(11), 2442–2444 (2005).
6. J. Peerlings, R. Riemenschneider, V. N. Kumar, M. Strassner, J. Pfeiffer, V. Scheuer, J. Daleiden, K. Mutamba, S. Herbst, H. L. Hartnagel, and P. Meissner, "Two-chip InGaAs-InP Fabry-perot p-i-n receiver for WDM systems," IEEE Photon. Technol. Lett. **11**(2), 260–262 (1999).
7. M. Oehme, J. Werner and E. Kasper, "High bandwidth Ge p-i-n photodetector integrated on Si," Appl. Phys. Lett. **89**, 071117–1– 071117–3 (2006).
8. L. Vivien, J. Osmond, J.-M. Fédéli, D. Marris-Morini, P. Crozat, J.-F. Damlencourt, E. Cassan, Y. Lecunff, and S. Laval, "42 GHz p.i.n Germanium photodetector integrated in a silicon-on-insulator waveguide," Opt. Express **17**(8), 6252–6257 (2009).
9. W. Y. Loh, J. Wang, J. D. Ye, R. Yang, H. S. Nguyen, K. T. Chua, J. F. Song, T. H. Loh, Y. Z. Xiong, S. J. Lee, M. B. Yu, G. Q. Lo and D, L, Kwong, "Impact of local strain from selective epitaxial germanium with thin Si/SiGe buffer on high-performance p-i-n photodetectors with a low thermal budget," IEEE Electron. Dev. Lett. **28**, 984–986 (2007).
10. L. Chen, and M. Lipson, "Ultra-low capacitance and high speed germanium photodetectors on silicon," Opt. Express **17**(10), 7901–7906 (2009).
11. D. Ahn, C. Y. Hong, J. F. Liu, W. Giziewicz, M. Beals, L. C. Kimerling, J. Michel, J. Chen, and F. X. Kärtner, "High performance, waveguide integrated Ge photodetectors," Opt. Express **15**(7), 3916–3921 (2007).
12. T. Yin, R. Cohen, M. M. Morse, G. Sarid, Y. Chetrit, D. Rubin, and M. J. Paniccia, "31 GHz Ge n-i-p waveguide photodetectors on Silicon-on-Insulator substrate," Opt. Express **15**(21), 13965–13971 (2007).

#120060 - $15.00 USD Received 16 Nov 2009; revised 27 Dec 2009; accepted 6 Jan 2010; published 25 Feb 2010

13. J. Wang, W. Y. Loh, K. T. Chua, H. Zang, Y. Z. Xiong, T. H. Loh, M. B. Yu, S. J. Lee, G. Q. Lo, and D. L. Kwong, "Evanescent-coupled Ge p-i-n photodetectors on Si-waveguide with SEG-GE and comparative study of lateral and vertical p-i-n configurations," IEEE Electron Device Lett. **29**(5), 445–448 (2008).
14. S. J. Koester, "J. D, Schaub, G. Dehlinger and J. O. Chu, "Germanium-on-SOI infrared detectors for integrated photonic application," IEEE J. Sel. Top. Quantum Electron. **12**, 1489–1502 (2006).
15. Q. Fang, J. F. Song, G. Zhang, M. B. Yu, Y. L. Liu, G. Q. Lo, and D. L. Kwong, "Monolithic integration of a multiplexer/demultiplexer with a thermo-optic VOA array on an SOI platform," IEEE Photon. Technol. Lett. **21**(5), 319–321 (2009).
16. Q. Fang, F. Li, and Y. L. Liu, "Compact SOI arrayed waveguide garting demultiplexer with broad spectral response," Opt. Commun. **258**(2), 155–158 (2006).
17. W. Tong, V. M. Menon, F. Xia, and S. R. Forrest, "An asymmetric twin waveguide eight-channel polarization-independent arrayed waveguide grating with an integrated photodiode array," IEEE Photon. Technol. Lett. **16**(4), 1170–1172 (2004).
18. M. Kohtoku, H. Sanjoh, S. Oku, Y. Kadota, and Y. Yoshikuni, "Packaged polarization-insensitive WDM monitor with low loss (7.3 dB) and wide tuning range (4.5nm)," IEEE Photon. Technol. Lett. **10**(11), 1614–1616 (1998).
19. M. Zirngibl, C. H. Joyner, and L. W. Stulz, "WDM receiver by monolithic integration of an optical preamplifier, waveguide grating router and photodiode array," Electron. Lett. **31**(7), 581–582 (1995).
20. S. Assefa, F. Xia, S. W. Bedell, Y. Zhang, and T. Topuria, P. M, Rice and Y. A. Vlasov, " CMOS-Integrated 40GHz Germanium Waveguide Photodetector for On-chip Optical Interconnects," Optical Fiber Communication Conference, OMR4 (2009).
21. G. Masini, L. Calace, G. Assanto, H. C. Luan, and L. C. Kimerling, "High-Performance p-i-n Ge on Si Photodetectors for the Near Infrared: From Model to Demonstration," IEEE Trans. Electron. Dev. **48**(6), 1092–1096 (2001).

1. Introduction

Wavelength division multiplexing (WDM) technology has been rapidly developed and widely deployed in optics communication system, due to its advantages of high reliability and high transmission capability [1–3]. WDM system enables multiple channel data transmission in a single fiber-optic link and can dramatically increase the aggregate data rate. However, WDM transmitters and receivers tend to be costly as the components for multiplexing/de-multiplexing, as well as the active components for each channel, have to be assembled together [4–6]. Furthermore, the size of the silica-based multiplexer/de-multiplexer (MUX/DEMUX) optical filter itself is large, with dimensions on the centimeter scale.

Silicon photonics has attracted much attention due to its advantages of low cost, high volume manufacturability and its compatibility with complementary metal oxide semiconductor (CMOS) technology. A major advantage of silicon photonics is the feasibility of monolithically integrating most of the electronic-photonic components on a single chip. This significantly reduces assembly processes, which can drastically reduce component sizes. The integration of Ge-on-Si photodetectors enables the detection of optical signals at 1.55 μm [7–14]. By utilizing a waveguided configuration instead of a surface illuminated configuration, Ge-on-Si photodetectors can achieve >40 GHz bandwidth and a responsivity of 1 A/W at 1550 nm [8]. However, it is challenging to realize a discrete Ge-on-Si photodetector that is capable of handling parallel data transmission due to its limited bandwidth. The WDM technology is an effective method to enhance the transmission capability of the receiver in optics communication. Arrayed Waveguide Grating (AWG) is one key component of WDM system and can be used to perform MUX/DEMUX functions [15,16]. In addition, due to the high index contrast between Si and SiO_2, the dimensions of the MUX/DEMUX can be shrunk many-fold when it is fabricated on silicon-on-insulator (SOI). In the past decades, integrated WDM receivers based on compound semiconductors materials have been reported [17–19]. However, compound semiconductor receivers incur very high cost which limits its widespread application. Due to the narrow bandgap of Ge, the absorption coefficient rolls off rapidly in the L-band wavelength range [14]. This imposes a huge challenge for Si photonics to be adopted for L-band communication applications. It is obvious that waveguided configuration will be necessary to boost the photodetection responsivity at L-band wavelengths, where the absorption coefficient of Ge is very low compared to C-band wavelengths.

#120060 - $15.00 USD Received 16 Nov 2009; revised 27 Dec 2009; accepted 6 Jan 2010; published 25 Feb 2010

In this work, a monolithically integrated silicon photonic WDM receiver chip was designed and fabricated. The receiver comprises of a 1 x 32 Si-based AWG and an array of high speed waveguided Ge-on-Si photodetectors on the SOI wafer with 300 nm top Si layer and 2 μm buried oxide (BOX). Due to the large index contrast between Si and SiO_2, the dimensions of the Si AWG can be reduced many-fold compared to silica counterparts. As such, the footprint of the AWG measures only about 400 μm × 500 μm. The AWG channel spacing is 200 GHz and each output channel of AWG is connected to a waveguided Ge-on-Si photodetectors (WGPD). In order to evaluate the feasibility of silicon photonics for L band communications, the WDM receiver was designed with 32 channels spanning from about 1570 to 1620 nm.

2. Design and Fabrication

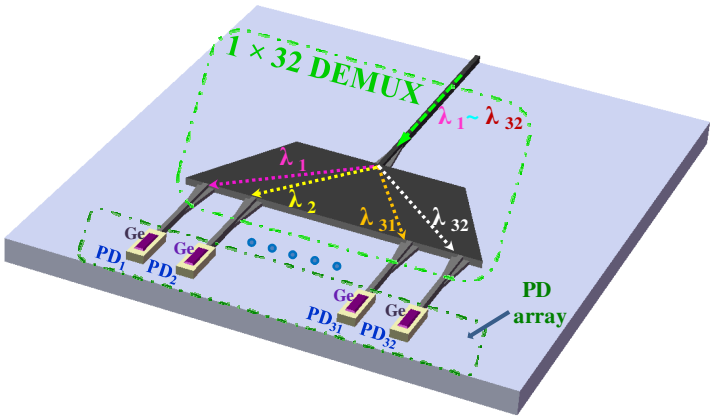

Fig. 1. The schematic of the WDM receiver composed of AWG and PD array

The schematic of the WDM receiver is shown in Fig. 1. It is composed of a DEMUX with 1 × 32 AWG and an array of Ge-on-Si vertical *p-i-n* waveguided photodetectors. A group of optical signals with 32 different wavelengths (λ_1~λ_{32}) are launched from the input waveguide of AWG. And then, the 32 optical signals are divided into 32 output channels of AWG, respectively. Then, each divided signal is coupled into a WGPD. We used the WDM_Phaser software from Optiwave Systems Inc. to design the AWG. In order to maintain single mode propagation in the waveguide and to reduce the crosstalk due to phase noise, ridge waveguides are designed as arrayed waveguides. A nano-taper was used as the mode-size converter at the input. In order to reduce the coupling loss between the nano-taper and the optical lensed fiber at the input while ensure mode confinement at the output, the ridge waveguides are gradually transited into channel waveguides at the input/output of the AWG. The channel waveguides are 500 nm wide and 300 nm tall while the ridge waveguides were similarly wide, with a slab thickness of 150 nm. The device is designed to operated at the grating order of 12, with a path length difference of 8.58 μm for the transverse-electric (TE) mode. And the free propagation region (FPR) focal lenth is 183 μm. The minimum pitch between the neighboring waveguides is 1.5 μm at the fan-out section. The minimum radius of arrayed waveguide is 10 μm. The bend loss with 10 μm radius is negligible. And this radius can make the AWG size small, so it can effectively reduce the transmission loss.The optical channel spacing of AWG is 200 GHz. In order to reduce the non-uniformity of optical loss, a broad free spectral range (FSR) of 74 nm is designed, which is larger than the necessary spectral range of 51.2 nm for the designed AWG. At the same time, more than 70 arrayed waveguides are designed to further reduce the transmission loss of AWG. It is easy to extend the number of output channels to form 1 × 46 AWG without any other modifications. Due to the high refractive index of Ge, 20 μm-long Ge on the 220nm-high Si waveguide can almost

#120060 - $15.00 USD Received 16 Nov 2009; revised 27 Dec 2009; accepted 6 Jan 2010; published 25 Feb 2010

completely absorb the optical signal at 1550 nm [20]. A Ge active area with a longer length will cause higher capacitance and dark current. In order to balance the receiver's speed, sensitivity and responsivity, the designed Ge active area on the 300 nm-high Si waveguide is 5 μm wide and 25 μm long in each of our photodetectors. The Ge thickness is 500 nm.

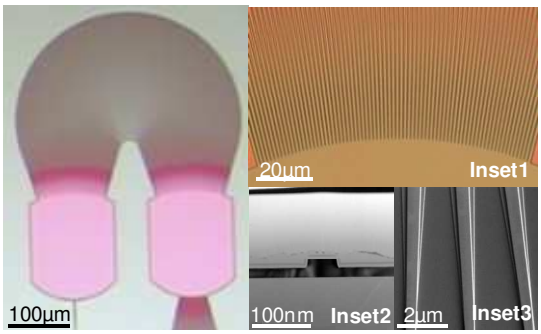

Fig. 2. Images of the processed AWG. Inset 1: Arrayed waveguides; Inset 2: Arrayed waveguide Cross-section; Inset 3: Output transition waveguides.

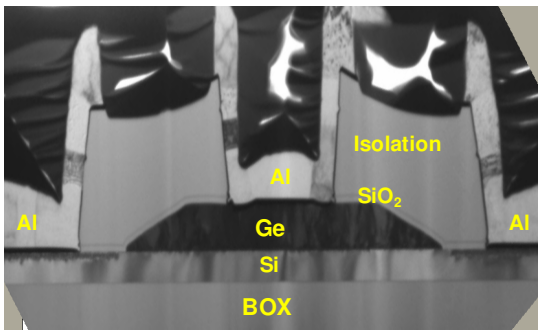

Fig. 3. TEM cross-section of the waveguided Ge-on-Si photodetector

The WDM receiver was fabricated on an 8-inch silicon-on-insulator (SOI) wafer with 300 nm top Si layer and 2 μm buried oxide (BOX). The ridge arrayed waveguides were formed by partially etching 150 nm of Si, shown in Fig. 2(Inset 2). The remaining 150 nm of Si was etched after a second lithography step to form the channel waveguides. Figure 2(Insert 3) shows the transition area from ridge waveguide to channel waveguide by double etching processes. AWG is formed after double Si etching processes. The microscope images of entire AWG are shown in Fig. 2 and it includes the input/output waveguides, input/output slab and arrayed waveguides. Figure 2(Inset 1) shows the arrayed waveguides at the fan-out section. To form the Ge photodetectors, separate masks were used to implant boron into the photodetector regions to form the *p* anode regions and the *p* + Ohmic contacts. The implants were activated via rapid thermal anneal of 1050 °C for 5 seconds prior to the selective epitaxial growth of Ge in an ultrahigh vacuum chemical vapor deposition (UHVCVD) epitaxy reactor. After depositing a thin layer of oxide, windows were opened in the Ge active regions by a combination of dry and wet etching to expose the underlying Si. After growing a thin SiGe buffer layer at 350 °C, Ge was selectively grown to a thickness of 500 nm at 550 °C. The *n* + ohmic contact was formed by implanting phosphorus into Ge, followed by an annealing at 500 °C for 5 min. For both of *p* + and *n* + Ohmic contacts, double implantations with different energies and doses were used to reduce the contact resistance. Then, a TaN/Al metal stack was deposited and etched to form top and bottom contacts after contact holes opening. Finally, more than 100 μm Si cavity was etched to hold optical lensed fiber for coupling with the nano-taper of Si waveguide, instead of a polishing process. The cross-section of WGPD is shown in Fig. 3.

#120060 - $15.00 USD Received 16 Nov 2009; revised 27 Dec 2009; accepted 6 Jan 2010; published 25 Feb 2010

3. Measured results

First, the performances of the stand-alone 1 × 32 AWG and Ge-on-Si photodetector were evaluated. As the actual AWG in the WDM receiver is terminated by Ge photodetectors, a stand-alone reference AWG with identical parameters was fabricated on the same chip, and was used for optical characterization. After dicing process, a polarization-maintaining (PM) lensed fiber with 2.5 μm spot diameter was used to couple the light into the nano-taper of the Si waveguide. The tip width of nano-taper is about 180 nm and the coupling loss between nano-taper and optical lensed fiber is about 2.5 dB/facet. The normalized power spectrum of transverse-electric (TE) for each of the 32 output waveguides is shown in Fig. 4. The power spectra were normalized by the transmission power spectrum of a short waveguide test structure, so as to decouple the coupling losses. The on-chip transmission loss of the AWG is 2.5 dB and the non-uniformity of transmitted power between all the channels was less than 3 dB. Good crosstalk performance of more than 18dB was obtained. In addition, the AWG also shows an additional advantage of having a wider bandwidth in its pass-band compared to other filter types such as ring resonators. The 1-dB bandwidth for each channel is about 40% of the channel spacing.

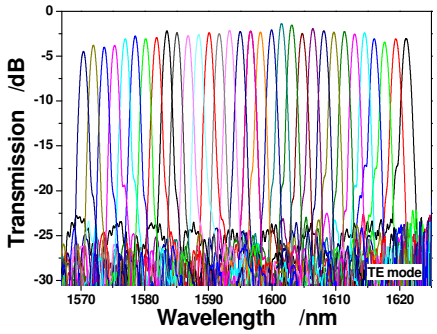

Fig. 4. Optical transmission spectra of the 1 × 32 Si AWG for TE mode

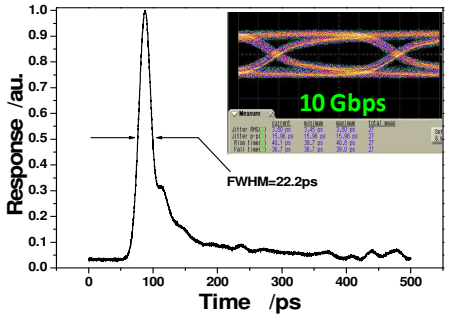

Fig. 5. Impulse response of photodetector at a bias of −1V and λ = 1550nm. 10 Gbps eye diagram is shown in the inset.

A stand-alone Ge photodetector was similarly used for high speed optical characterization so that the effects of the trans-impedance amplifier (TIA) can be decoupled. The impulse response of the reference WGPD is plotted in Fig. 5, with the 10 Gbps eye diagram shown in the inset. The maximum bit-rate of 10 Gbps was limited by our test equipment. The measured pulse shows a full-width at half maximum (FWHM) of only 22.2 ps, indicating that an even higher data rate is possible, although operating at bandwidth extremes will come with sensitivity trade-offs.

#120060 - $15.00 USD Received 16 Nov 2009; revised 27 Dec 2009; accepted 6 Jan 2010; published 25 Feb 2010

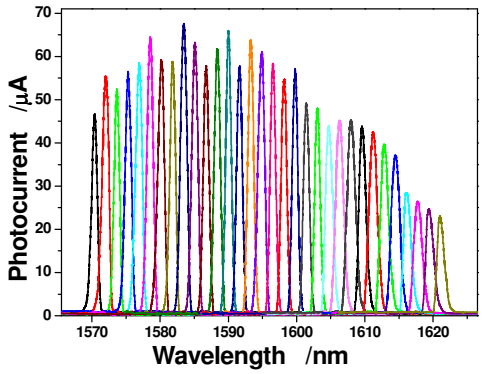

Fig. 6. Photocurrent spectra of WDM receiver at −7.5dBm optical power entering input waveguide

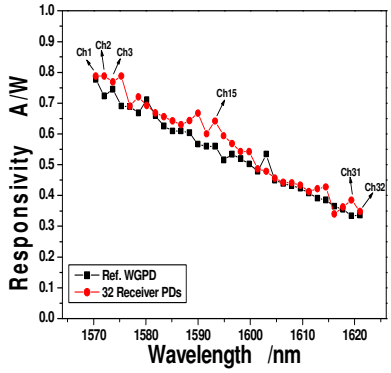

Fig. 7. Responsivity of each WGPD of the 32 channels of the DWDM receiver, showing good agreement with the responsivity of the reference stand-alone WGPD.

The photocurrent spectrum of each channel of the WDM receiver is collected by scanning the input optical wavelength at the bias of −1 V. The photocurrent spectra of 32 channels of the WDM receiver are plotted in Fig. 6. The optical power entering the input waveguide of the WDM receiver is about −7.5 dBm, with the input coupling loss decoupled. The dark current of the Ge PD is less than 1 μA and the crosstalk is more than 15 dB, which is closed to the result of reference AWG tested by the external photodetector. The channel spacing of the WDM receiver is about 200 GHz. The photocurrent non-uniformity of the WDM receiver is about 4.5 dB, more than the optical non-uniformity of the reference AWG. This is due to the absorption coefficient rolls off in L-band wavelgnth regime [14]. Based on the photocurrent spectra, the WGPD responsivity for all 32 channels of the WDM receiver is plotted in Fig. 7, together with that of the stand-alone WGPD. The responsivity values agree well with that of the stand-alone WGPD. At a bias of −1V, the responsivity decreases gradually with increasing wavelength. The results show that by virtue of its long absorption region, the WGPD still exhibits a responsivity of 0.33 A/W even at 1620 nm. For the surface illuminated Ge photodetectors with 1 μm Ge thickness, the responsivity is only ~0.3 and ~0.03 A/W at 1550 and 1620 nm, respectively [21].

#120060 - $15.00 USD Received 16 Nov 2009; revised 27 Dec 2009; accepted 6 Jan 2010; published 25 Feb 2010

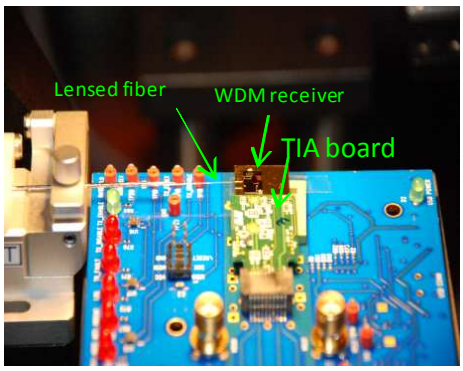

Fig. 8. Experimental setup with TIA board for the BER measurement

The WDM receiver chip is packaged with the transimpedance amplifier (TIA) on an electrical evaluation board to enable sensitivity measurement. The measurement setup with TIA is shown in Fig. 8. The bias from the TIA into the photodetector is also −1 V. Figure 9 shows the 10 Gbps eye diagram of the WDM receiver (channel 1) at the transimpedance amplifier (TIA) output. It is observed that the TIA adds a significant amount of jitter and other waveform artifacts, which is obvious when compared to the direct output from the WGPD (Fig. 5 inset). Next, the bit error rate (BER) of channel 1 is measured for decreasing input optical power using a 2^{31}-1 pseudorandom bit sequence (Fig. 10(Left)). At the same time, according to the photocurrent spectra of the WDM receiver, the optical input sensitivity of the WDM receiver is extracted to be between −16 to −19 dBm for all 32 channels in the L band at a bit error rate (BER) of 1×10^{-11}. Figure 10(Right) shows the degradation of BER when the optical wavelength is intentionally deviated from the central wavelength, λ_1 (pass-band maxima). The BER degrades from ~10^{-12} to ~10^{-8} when the deviation is +/−0.3 nm from λ_1 at an input optical power of −18.7dBm. The results agree well with the 1-dB bandwidth of the AWG's pass-band. At the same time, it also highlights the importance of having a wide pass-band in order to maximize the input sensitivity across all channels.

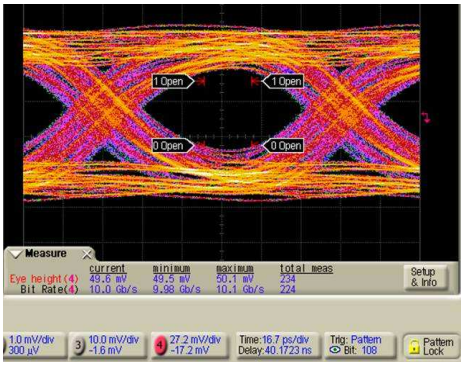

Fig. 9. 10 Gbps eye diagram of the DWDM receiver (channel 1). Significant jitter and waveform artifacts are added by the TIA. BER at this input optical power is better than 10^{-12}.

#120060 - $15.00 USD Received 16 Nov 2009; revised 27 Dec 2009; accepted 6 Jan 2010; published 25 Feb 2010

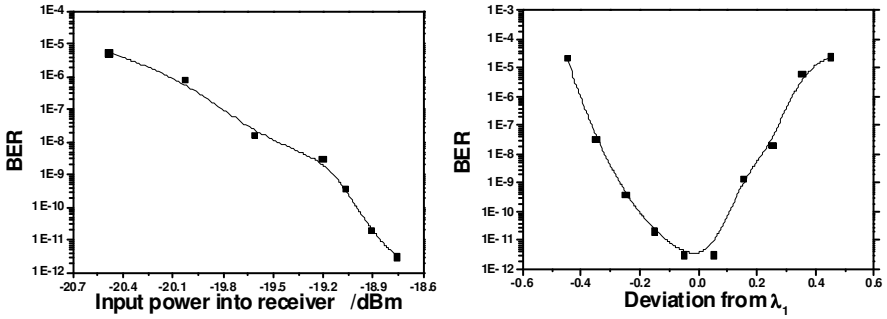

Fig. 10. (Left) BER vs. input optical power at the central wavelength of channel 1, λ_1; (Rignt) BER vs. wavelength deviation from λ_1

In conclusion, a high performance WDM receiver with 32 channels has been implemented using silicon photonics technology. It is composed of 1 × 32 AWG and Ge-on-Si waveguided photodetector array. The Si-based AWG has 200 GHz channel spacing and optical crosstalk performance of more than 18 dB. With each channel being capable of operating at a data rate of at least 10 Gbps, the aggregate data rate of the WDM receiver is at least 320 Gbps. At a BER of 1×10^{-11}, the WDM receiver showed an optical input sensitivity between −16 dBm and −19 dBm for all 32 channels in Lband. This first demonstration indicates the feasibility and potential of manufacturing low cost silicon WDM receivers for terabit data communications.

#120060 - $15.00 USD Received 16 Nov 2009; revised 27 Dec 2009; accepted 6 Jan 2010; published 25 Feb 2010